

SPATIALLY STRUCTURED ACTIVITY IN SYNAPTICALLY COUPLED NEURONAL NETWORKS: II. LATERAL INHIBITION AND STANDING PULSES*

DAVID J. PINTO[†] AND G. BARD ERMENTROUT[‡]

Abstract. We consider the existence and stability of standing pulse solutions to a system of integro-differential equations used to describe the activity of synaptically coupled networks of excitatory and inhibitory neurons in a single spatial domain. Assuming an arrangement of synaptic connections described by “lateral inhibition,” previous formal arguments have demonstrated the existence of both stable and unstable standing pulses [S. Amari, *Biol. Cybern.*, 27 (1977), pp. 77–87]. These results have formed the basis for several recent hypotheses regarding the generation of sustained activity patterns in prefrontal cortex and other brain regions. Implicit in the lateral inhibition arrangement, however, is the assumption that the dynamics of inhibition are instantaneous. Here we present two arguments demonstrating the loss of stability of standing pulse solutions through a Hopf bifurcation when more realistic inhibitory dynamics are considered. The first argument parallels Amari’s formal presentation, while the second provides a rigorous analysis of the linearized system. Additionally, we extend the existence of solutions to include a broader range of conditions by constructing a standing pulse using singular perturbation analysis.

Key words. synaptic networks, cortical activity, stability analysis, singular perturbation

AMS subject classification. 92C20

PII. S0036139900346465

1. Introduction. Lateral inhibition (LI) first gained broad acceptance as a mechanism for neuronal processing through a series of reports on the retina of the horseshoe crab *Limulus polyphemus* (for review, see [18]). The Limulus retina is composed of a lattice of light-sensitive units, each having a direct inhibitory effect on its neighbors; the effect is weak for nearest neighbors, stronger for units separated by some distance, and negligible for pairs more than 8–10 units apart. The dynamics of this inhibition are such that effects may be delayed for up to 200 ms, independent of the spatial separation between pairs.

Several studies have examined theoretically the dynamics of activity in LI networks [33], [3], [36], [37], [29], [1], [34]. Typically, networks are considered in which nearby neurons excite each other, while more distant pairs have an inhibitory effect (for review, see [13]). In contrast to studies in the Limulus retina, the effects of inhibitory delays or temporal differences between excitation and inhibition are not usually considered in detail (however, see [7]).

An early finding from the analysis of LI networks is that they admit standing pulse solutions, i.e., regions of excitatory activity sustained in the absence of external drive. The existence and stability of such solutions were demonstrated numerically in [34] and, under certain simplifying assumptions, proven analytically in [1]. More recently, it has been suggested that a similar set of network dynamics may be involved in the sustained activity recorded from neurons in prefrontal cortex during the delay

*Received by the editors July 5, 2000; accepted for publication (in revised form) March 2, 2001; published electronically August 22, 2001. This research was supported by grants from NSF, NIMH, and NIH.

<http://www.siam.org/journals/siap/62-1/34646.html>

[†]Department of Neuroscience, Brown University, Providence, RI 02912 (dpinto@bu.edu).

[‡]Department of Mathematics and Department of Neurobiology, University of Pittsburgh, Pittsburgh, PA 15261 (bard@pitt.edu).

period of a delayed-response task [3], [2], [16].

In the present study, we investigate the ability of LI networks to maintain stable standing pulse solutions in the presence of more realistic inhibitory delays. In particular, we examine the existence and stability of standing pulse solutions to an integro-differential equation system used to describe neuronal activity in a synaptically coupled network of excitatory and inhibitory neurons along a single spatial domain:

$$(1) \quad \begin{aligned} u_t &= -u + \int_{-\infty}^{\infty} w_{ee}(x-x')P_e(u(x',t) - \theta)dx' \\ &\quad - \int_{-\infty}^{\infty} w_{ie}(x-x')P_i(v(x',t) - \theta)dx', \\ \tau v_t &= -v + \int_{-\infty}^{\infty} w_{ei}(x-x')P_e(u(x',t) - \theta)dx' \\ &\quad - \int_{-\infty}^{\infty} w_{ii}(x-x')P_i(v(x',t) - \theta)dx'. \end{aligned}$$

Here, u and v represent the average level of activity (e.g., voltage) in a population of excitatory (e) and inhibitory (i) neurons, respectively, at spatial point x and time t ; w_{jk} is the distance-dependent kernel representing the strength or “weight” of connectivity from population j to population k ($j, k \in \{e, i\}$); τ is the inhibitory time constant; and P_j is the synaptic firing rate, which depends on the activity in population j relative to some constant threshold θ .

A more detailed description of the equations and underlying assumptions is presented below in section 2. In particular, we show that using an LI weight kernel that neglects inhibitory dynamics carries the implicit assumption that inhibitory mechanisms act instantaneously. In section 3, we review previous arguments for the existence of standing pulse solutions and then employ a singular perturbation approach to construct solutions under different circumstances. Interestingly, both the inner and outer layers of the perturbation analysis involve a convolution operator, requiring both sets of solutions to be considered globally. In section 4, we review a previous formal argument for the stability of standing pulse solutions and then present two arguments demonstrating the loss of stability when more realistic inhibitory dynamics are considered. The first is a formal argument that parallels Amari’s strategy. The second is a rigorous analysis examining the eigenvalues of the linearized system. In section 5, we summarize our results and discuss their implications for understanding neuronal processing in prefrontal cortex and other brain regions.

2. Mathematical assumptions. In the analysis which follows, we assume that the firing rate function for the inhibitory population (P_i) is linear and denote the excitatory function, P_e , as simply P . This renders the equations slightly less general but is in fact a reasonable assumption, supported by experimental data comparing the firing properties of excitatory versus inhibitory neurons in neocortex [24]. In addition, for simplicity of exposition, we neglect the term describing recurrent inhibition ($i \rightarrow i$), although much of the analysis would proceed unaltered were it included. Under these assumptions, (1) becomes

$$(2) \quad \begin{aligned} u_t &= -u + \int_{-\infty}^{\infty} w_{ee}(x-x')P(u(x',t) - \theta)dx' - \int_{-\infty}^{\infty} w_{ie}(x-x')v(x',t)dx', \\ \tau v_t &= -v + \int_{-\infty}^{\infty} w_{ei}(x-x')P(u(x',t) - \theta)dx'. \end{aligned}$$

We consider the functions w_{ij} to be defined on $(-\infty, \infty)$ as bounded, nonnegative, even, and normalized such that $\int_{-\infty}^{\infty} w_{ij}(x)dx = 1$. As an example, consider $w(x) = 1/2b e^{-|x|/b}$ or $w(x) = 2\sqrt{b/\pi}e^{-bx^2}$, where $b > 0$ is a measure of the synaptic “footprint.” The function P is defined on $[0, 1]$, monotonic increasing, $P'(0) < 1$, $P'(1) < 1$, and such that the function $f(u) \equiv -u + P(u)$ has precisely three zeros, typically at or near $u = 0$, k , and 1, with $0 < k < 1$. As an example, consider $P(u - \theta) = \frac{1}{2}(1 + \tanh(\beta(u - \theta)))$, or, as a limiting case ($\beta \rightarrow \infty$), $P(u - \theta) = H(u - \theta)$, where $H(x) = 0$ for $x < 0$, $H(x) = 1$ for $x \geq 0$. Here, θ is some constant threshold value ($0 < \theta < 1$). We will employ the result of [12] establishing the existence of traveling front solutions under the above conditions on w , P , and in the absence of inhibition ($v \equiv 0$), e.g., solutions of the form $u(x, t) = U(x - ct)$, monotonic decreasing, $U(-\infty) = 1$, $U(\infty) = 0$, with c of constant value.

As described above, many previous studies have considered networks with direct LI, employing a single kernel in which nearby regions exert a positive influence while more distant regions have an inhibitory effect. Anatomical results, on the other hand, suggest that it is the excitatory projections that extend across long distances, while inhibitory connections tend to remain more local [21], [15]. This seeming contradiction is resolved by recognizing that network models using direct LI implicitly assume that inhibition acts instantaneously. In (2), for instance, with instantaneous inhibition (i.e., $\tau = 0$) we solve the second equation for v and substitute into the first to obtain

$$(3) \quad u_t = -u + (w_{ee} - w_{ie} * w_{ei}) * P(u - \theta).$$

(For clarity, the notation $f * g \equiv \int_{-\infty}^{\infty} f(x - y)g(y)dy$ will be used where appropriate.) Assuming that the excitatory projections extend equally to both populations (i.e., w_{ee} and w_{ei} have the same footprint [35]), the resulting kernel indeed describes direct LI. Figure 1 illustrates the generation of LI from anatomically correct patterns of excitatory and inhibitory connections.

3. Existence of standing pulses. This section explores the existence of standing pulse solutions in LI networks, i.e., regions in which activity is sustained in the absence of external input. More formally, we consider standing pulses as stationary solutions of (2) (or, equivalently, (3)) of the form $u(x, t) = U(x)$, $U(\pm\infty) = 0$, $U(a_1) = U(a_2) = \theta$, where $0 < \theta < 1/2$, $U(x) < \theta$ for $x > a_2$ and $x < a_1$, and $\Phi = a_2 - a_1$ describes the width of the pulse (cf. Figure 2b). Note that because we are examining steady state solutions, the dynamics of excitation and inhibition are not relevant, so that direct LI may be assumed.

3.1. Amari’s argument for pulse existence. If, in addition to LI, we assume that the firing rate can be described using the Heaviside function, $H(u - \theta)$, then it is straightforward to establish the existence of standing pulse solutions. We present, in brief, an argument first described by Amari [1].

Let $w(x)$ describe a direct lateral inhibition kernel (Figure 1). Note that steady state solutions of (3) satisfy

$$u(x) = \int_{-\infty}^{\infty} w(x - x')H(u(x') - \theta)dx',$$

which, in the case of a standing pulse solution, reduces to,

$$u(x) = \int_{a_1}^{a_2} w(x - x')dx'.$$

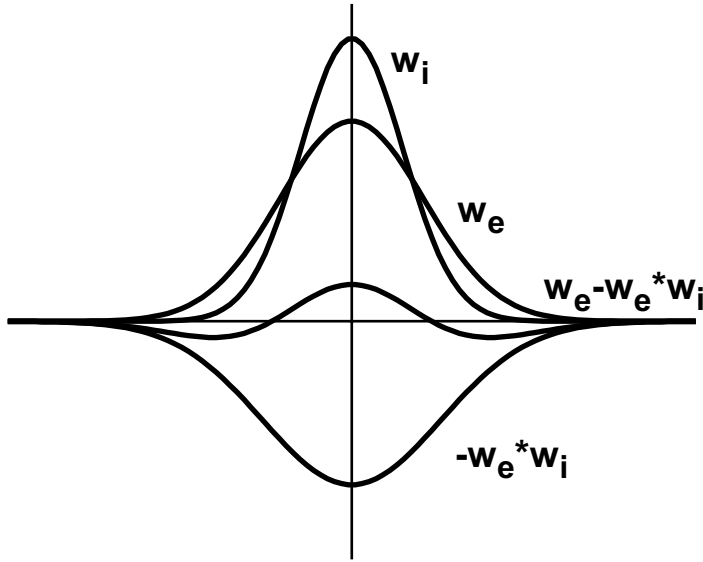


FIG. 1. *Lateral Inhibition.* Anatomically, the extent of excitatory connections (w_e) is broader than that of inhibitory connections (w_i). The extent of indirect inhibition ($w_e * w_i$) is broader than either type of direct connection alone. The net result is a pattern of influence described by lateral inhibition ($w_e - w_e * w_i$). However, as described in the text, this pattern is valid only under the assumption that inhibition acts instantaneously.

Moreover, at $x = a_1$,

$$\begin{aligned}\theta &= \int_{a_1}^{a_2} w(a_1 - x') dx' \\ &= \int_0^{a_2 - a_1} w(s) ds \\ &\equiv G(a_2 - a_1),\end{aligned}$$

where $G(\Phi) \equiv \int_0^\Phi w(y) dy$, and we have used the fact the w is even.

To construct a solution, we must show that there is a root to the equation $G(\Phi) = \theta$; this root corresponds to the width of a stationary pulse. Since the system is translation invariant, the center of the pulse can occur anywhere on the real line. Only the width must be computed. The graph of G for a typical kernel, w , reveals that, in fact, two pulse solutions exist over a range of thresholds, θ , one narrow and one wide (Figure 2(a)). As θ increases, the narrow and wide pulses converge and vanish.

3.2. Singular perturbation construction. We now return to more general nonlinearities, P . We will use a singular perturbation argument to construct a standing pulse by assuming that the footprint of the inhibition is much larger than that of the excitation. We will assume that the more general firing rate functions P satisfy the criteria for the existence of traveling fronts as in [12] and summarized above.

Let $1/\epsilon$ be the footprint for inhibition where $\epsilon \ll 1$. With this assumption, (2) becomes

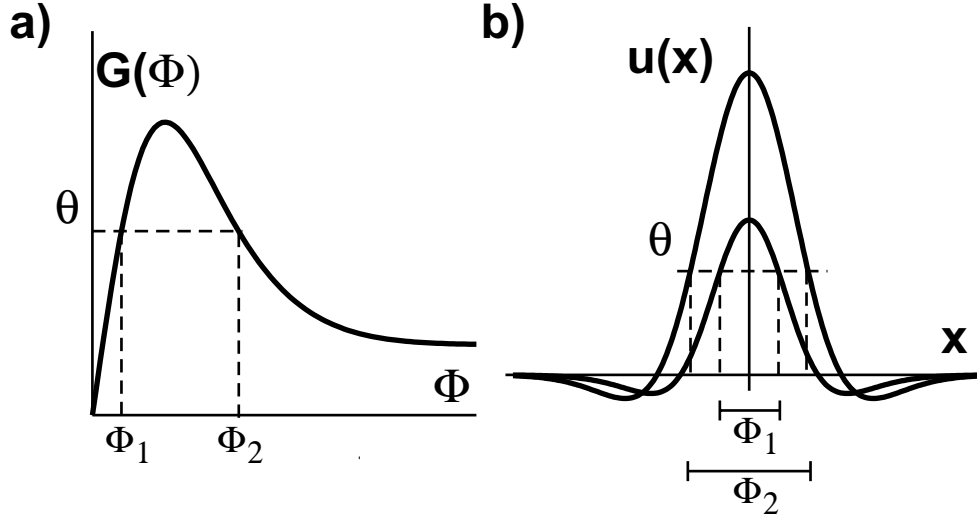


FIG. 2. Schematic of Amari's construction of stable standing pulses. (a) The pulse width function $G(\phi) = \theta$ has two roots, ϕ_1 and ϕ_2 , corresponding to the two standing pulse solutions shown in (b).

$$\begin{aligned}
 0 &= -u + \int_{-\infty}^{\infty} w_e(x-x')P_1(u(x') - \theta)dx' - \epsilon \int_{-\infty}^{\infty} w_i(\epsilon(x-x'))v(x')dx', \\
 (4) \quad 0 &= -v + \int_{-\infty}^{\infty} w_e(x-x')P_2(u(x') - \theta)dx',
 \end{aligned}$$

where, for clarity of exposition, we take $w_{ee} = w_{ei} \equiv w_e$, $w_{ie} \equiv w_i$, and, to be slightly more general, we allow P_1 to differ from P_2 , although both satisfy the appropriate conditions for a firing rate function.

The inner, or narrow, equations are obtained by allowing $\epsilon \rightarrow 0$, which yields

$$\begin{aligned}
 0 &= -u(x) + (w_e * P_1(u - \theta))(x) - v(\bar{x}), \\
 0 &= -v(x) + (w_e * P_2(u - \theta))(x),
 \end{aligned}$$

where $v(\bar{x})$ is a constant described below. For the outer, or broad, equations we compress space with the change of variable $\xi = \epsilon x$ to get

$$\begin{aligned}
 0 &= -u(\xi) + 1/\epsilon \int_{-\infty}^{\infty} w_e(1/\epsilon(\xi - \xi'))P_1(u(\xi') - \theta)d\xi' - \int_{-\infty}^{\infty} w_i(\xi - \xi')v(\xi')d\xi', \\
 0 &= -v(\xi) + 1/\epsilon \int_{-\infty}^{\infty} w_e(1/\epsilon(\xi - \xi'))P_2(u(\xi') - \theta)d\xi'
 \end{aligned}$$

and then let $\epsilon \rightarrow 0$ to obtain

$$\begin{aligned}
 0 &= -u(\xi) + P_1(u(\xi) - \theta) - (w_i * v)(\xi), \\
 0 &= -v(\xi) + P_2(u(\xi) - \theta).
 \end{aligned}$$

Here we have employed the fact that, for a Gaussian-like kernel w ,

$$\lim_{\epsilon \rightarrow 0} \frac{1}{\epsilon} w\left(\frac{(\xi - \xi')}{\epsilon}\right) \rightarrow \delta(\xi - \xi'),$$

where $\delta(x)$ is the Dirac delta function.

Regions in which solutions are described by the narrow equations will be handled by appealing to the existence of traveling pulse solutions as described in [12]. Because inhibition is spatially distributed, and the outer equations involve a spatial convolution, the outer solutions must be considered globally rather than locally, as is the case for singular perturbation analysis of differential equations.

The space-clamped phase-plane is useful for describing the construction process (Figure 3). Beginning with the inner equations, we apply the existence results of Ermentrout and McLeod to construct a pair of front solutions describing the up and down jumps of the standing pulse, occurring at spatial points $-\bar{x}$ and \bar{x} , say (Figures 3(a) and 3(b)). As discussed in their study, the speed, c , of these fronts satisfies

$$c = \frac{-\int_{g_-(v(\bar{x}))}^{g_+(v(\bar{x}))} (-u - v(\bar{x}) + P_1(u - \theta)) du}{\int_{-\infty}^{\infty} (u')^2 P_1'(u - \theta) dz},$$

where $g_{\pm}(v)$ describes u as a function of v along the appropriate branch of $(-u + P(u - \theta))^{-1}$ (see Figure 3(a)). Since we require a pulse that is stationary, the points $\pm\bar{x}$ are determined such that the speed of the fronts is zero, i.e., $v(\bar{x}) = \mu$, where μ satisfies $\int (-u + P_1(u - \theta) - \mu) du = 0$. Note that the value of μ depends on the specific shape of P_1 .

The term $v(\bar{x})$ in the inner equation corresponds to the term $(w_i * v)(\bar{\xi})$ in the outer equation or, using the second of the outer equations, $(w_i * P_2(u - \theta))(\bar{\xi})$, where $\bar{\xi} = \epsilon\bar{x}$. Moreover, since $(w_i * P_2(u - \theta))(\xi) = -u + P_1(u - \theta)$, we consider solutions to the outer equations of the form

$$u = \begin{cases} u^+, & |\xi| < \bar{\xi}, \\ u^-, & |\xi| > \bar{\xi}, \end{cases}$$

where $u^+ = g_+(v(\xi))$ and $u^- = g_-(v(\xi))$. Note that such solutions are composed of an upper portion, u^+ , and a lower portion, u^- , and match the values of the inner solution at \bar{x} and $-\bar{x}$.

To complete the construction we must show that there exists some \bar{x} that satisfies $(w_i * P_2(u - \theta))(\bar{\xi}) = \mu$, where u is the solution to the outer equation described above. Less formally, we require a value for \bar{x} so that the solution, u , described by the outer equation (which depends on \bar{x} ; see Figure 3(b)) returns the ‘‘correct’’ value when passed through the convolution $(w_i * P_2(u - \theta))(\bar{\xi})$. This correct value, μ , is just the one that ensures that front solutions produced by the inner equations remain stationary.

The conditions under which such values for \bar{x} exist depend on the shapes of P_1 and P_2 . The exact nature of this dependence has yet to be determined. However, we may begin to understand the conditions by first considering the case in which P_2 is very sharp, and hence constant on the two domains ($P_2(u^+ - \theta) = v^+$, $P_2(u^- - \theta) = v^-$; see Figure 3(c)). In this case,

$$\begin{aligned} (w_i * P_2(u - \theta))(\xi) &= \int_{-\bar{\xi}}^{\bar{\xi}} w_i(\xi - \xi') P_2(u^+(\xi') - \theta) d\xi' \\ &\quad + \left(\int_{-\infty}^{-\bar{\xi}} + \int_{\bar{\xi}}^{\infty} \right) w_i(\xi - \xi') P_2(u^-(\xi') - \theta) d\xi', \\ (5) \qquad \qquad \qquad &= v^+ \phi(\xi) + v^- (1 - \phi(\xi)), \end{aligned}$$

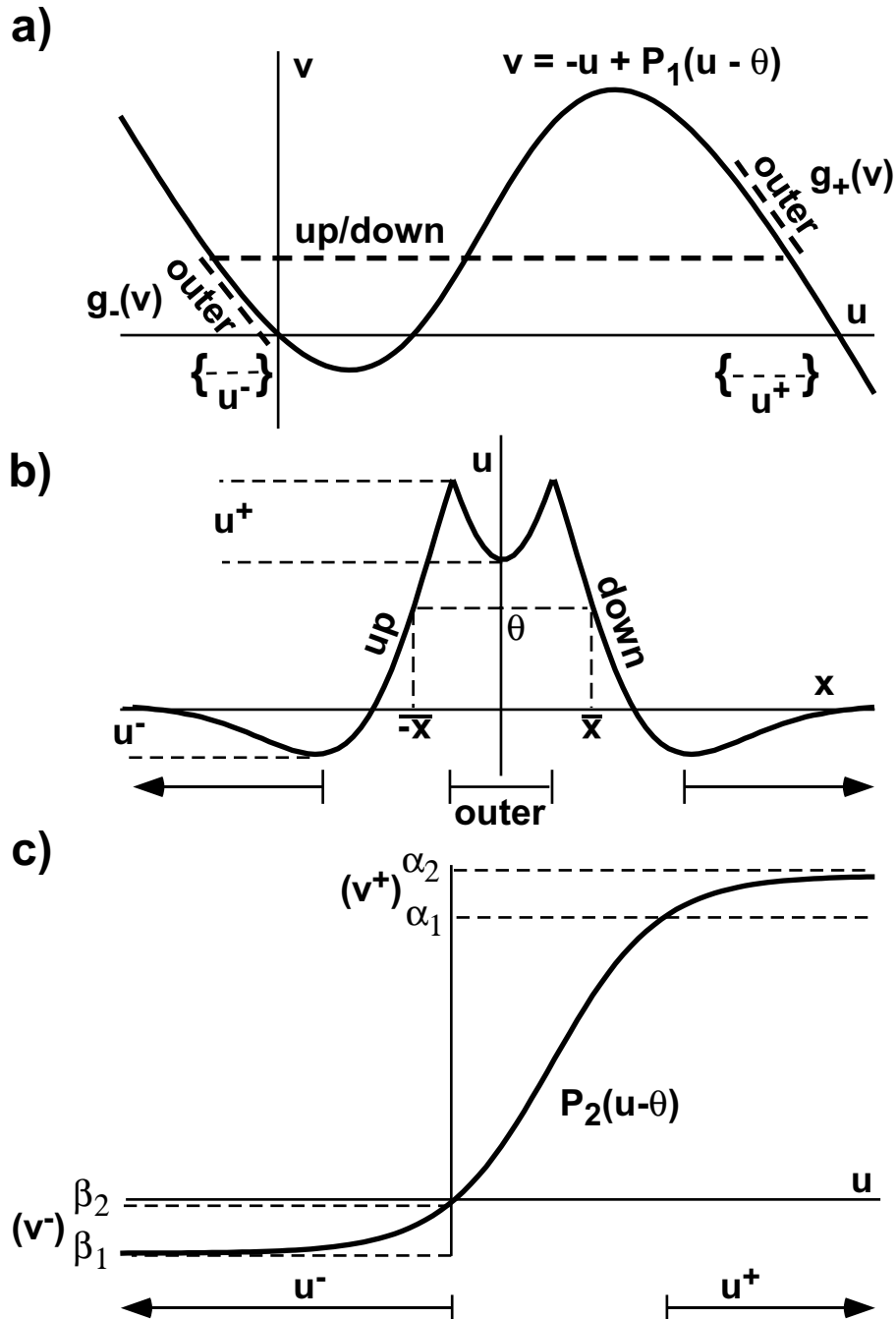


FIG. 3. Schematic of singular perturbation construction for standing pulses. (a) Space-clamped phase-plane illustrating the construction of the standing pulse shown in (b) from narrow up and down inner front solutions and a broad outer solution consisting of plateau and recovery portions. (c) Graph showing the dependence of up and down jump points on the shape of the firing function, $P(u - \theta)$ (see text).

where $\phi(\xi) \equiv \int_{\xi-\bar{\xi}}^{\xi+\bar{\xi}} w(y)dy$. Then \bar{x} is defined by satisfying

$$\mu = v^+ \phi(\epsilon \bar{x}) + v^- (1 - \phi(\epsilon \bar{x})).$$

As \bar{x} ranges over $[0, \infty)$, $\phi(\epsilon \bar{x}) = \phi(\bar{\xi}) = \int_0^{2\bar{\xi}} w(y)dy$ spans the interval $[0, 1/2]$. Thus, so long as

$$v^- \leq \mu \leq \frac{1}{2}(v^- + v^+),$$

we are guaranteed that the required \bar{x} can be found.

More generally, with no steepness conditions imposed on P_2 , we find values $\alpha_{1,2}$ and $\beta_{1,2}$ such that

$$\begin{aligned} \alpha_1 &\leq P_2(u^+ - \theta) \leq \alpha_2, \\ \beta_1 &\leq P_2(u^- - \theta) \leq \beta_2 \end{aligned}$$

(Figure 3(c)). Then, using the same strategy as above, we obtain the inequality

$$\alpha_1 \phi(\bar{\xi}) + \beta_1 (1 - \phi(\bar{\xi})) \leq (w_i * P_2(u - \theta))(\bar{\xi}) \leq \alpha_2 \phi(\bar{\xi}) + \beta_2 (1 - \phi(\bar{\xi}))$$

which, for $\bar{x} = 0$, yields

$$\beta_1 \leq (w_i * P_2(u - \theta))(\bar{\xi}) \leq \beta_2$$

and, for $\bar{x} = \infty$,

$$\frac{1}{2}(\alpha_1 + \beta_1) \leq (w_i * P_2(u - \theta))(\bar{\xi}) \leq \frac{1}{2}(\alpha_2 + \beta_2).$$

Thus, $(w_i * P_2(u - \theta))(\bar{\xi})$ spans values at least over the interval $[\beta_2, 1/2(\alpha_1 + \beta_1)]$, and a solution is guaranteed so long as

$$\beta_2 \leq \mu \leq \frac{1}{2}(\alpha_1 + \beta_1).$$

It remains to show that solutions to the outer equation vanish at $\pm\infty$. By symmetry, we need consider only the behavior of the solutions as $x \rightarrow +\infty$.

For ξ just beyond $\bar{\xi}$, $u = u^-$ lies in the domain of the lower branch and has a negative value. We show that, as ξ increases, u^- increases, and solutions follow the lower branch asymptotically into zero.

Starting from the outer equation and differentiating,

$$\begin{aligned} 0 &= -u(\xi) + P_1(u(\xi) - \theta) - (w_i * P_2(u - \theta))(\xi), \\ 0 &= -u'(\xi) + P_1'(u(\xi) - \theta)u'(\xi) - (w_i' * P_2(u - \theta))(\xi), \\ u'(\xi) &= -\frac{(w_i' * P_2(u - \theta))(\xi)}{1 - P_1'(u(\xi) - \theta)}. \end{aligned}$$

On the lower branch, we note that $P_1'(u - \theta)$ is positive but small, so that the denominator is always positive. The numerator, as in (5), becomes

$$\begin{aligned} w_i' * P_2(u - \theta) &= \int_{-\bar{\xi}}^{\bar{\xi}} w_i'(\xi - \xi') P_2(u^+(\xi') - \theta) dx' \\ &\quad + \left(\int_{-\infty}^{-\bar{\xi}} + \int_{\bar{\xi}}^{\infty} \right) w_i'(\xi - \xi') P_2(u^-(\xi') - \theta) d\xi'. \end{aligned}$$

For simplicity, we consider the case in which $P_2(u^\pm - \theta) \approx v^\pm$ and v^+ is sufficiently large compared to v^- , so that the expression is dominated by the first integral. The general case follows similarly but with a more complicated argument. In addition, we consider w satisfying the conditions stated above and also that $w(x)$ decreases as $|x|$ increases (e.g., $w(x) = 1/2b e^{-|x|/b}$; see [17] for more general connectivity patterns). Under these conditions we obtain the inequality

$$\begin{aligned} (w'_i * P_2(u))(\xi) &\approx v^+ \int_{-\bar{\xi}}^{\bar{\xi}} w'_i(\xi - \xi') d\xi' \\ &= v^+ \int_{\xi - \bar{\xi}}^{\xi + \bar{\xi}} w'_i(y) dy \\ &= v^+ (w(\xi + \bar{\xi}) - w(\xi - \bar{\xi})) \\ &< 0 \quad \text{for } \xi > \bar{\xi}. \end{aligned}$$

Thus $u'(\xi) > 0$ for $\xi > \bar{\xi}$, and u^- increases along the lower branch as required.

Finally, we note that, in contrast to the two pulse solutions derived using Amari’s argument, the singular perturbation construction results in only one solution. This can be understood intuitively by examining the widths of the two pulse solutions described in Figure 2. As $w(x)$ becomes tall and narrow with decreasing ϵ , the initial rise of G becomes steeper and the narrow pulse becomes more narrow, ultimately vanishing as w_{ee} approaches $\delta(x)$.

4. Stability of standing pulses. This section examines the dependence of the stability of pulse solutions on the dynamics of inhibition. Beginning with (3), we review Amari’s formal argument for stability and then extend the strategy to analyze the same solutions in a system that incorporates more realistic inhibitory dynamics. Next, a rigorous argument is presented that entails linearization about steady state pulse solutions and examining the dependence of the resulting eigenvalues on the time constant of inhibition.

4.1. Amari’s argument for pulse stability. Note that each of the two pulse solutions described in section 3.1 has exactly two points at which the average activity just reaches threshold. Let a_j ($j = 1, 2$) be such that $u(a_j, t) = \theta$; we then track the dynamic behavior of these points with

$$\frac{d}{dt}u(a_j(t), t) = u_x(a_j, t) \frac{da_j}{dt} + u_t(a_j, t) = 0.$$

Approximating $u_x(a_j(t), t)$ by its steady state value, say α ,

$$\begin{aligned} \alpha \frac{da_1}{dt} &= u(a_1(t), t) - \int_{-\infty}^{\infty} w(a_1 - x') H(u(x', t) - \theta) dx' \\ &= \theta - \int_{-\infty}^{\infty} w(a_1 - x') H(u(x', t) - \theta) dx'. \end{aligned}$$

Similarly,

$$\alpha \frac{da_2}{dt} = -\theta + \int_{-\infty}^{\infty} w(a_2 - x') H(u(x', t) - \theta) dx'.$$

Subtracting and simplifying,

$$\alpha \frac{d}{dt}(a_2 - a_1) = -2\theta + 2 \int_0^{a_2 - a_1} w(y) dy$$

reduces the system to a single equation describing the pulse width, with $\Phi \equiv a_2 - a_1$:

$$\frac{\alpha}{2} \frac{d\Phi}{dt} = -\theta + G(\Phi),$$

where, as before, $G(\Phi) \equiv \int_0^\Phi w(y)dy$.

As in the existence argument of section 3.1, a sketch of G reveals two steady state solutions over a range of thresholds, θ : a narrow pulse of width Φ_1 , and a wide pulse of width Φ_2 (Figure 2(a)). From the same sketch, we note that $G'(\Phi_1) > 0$ and $G'(\Phi_2) < 0$, making it immediately apparent that the outer pulse is stable while the inner is unstable.

As an aside, note that as θ decreases, the width of the wide pulse increases to infinity, essentially transforming the pulse into a pair of traveling fronts moving in opposite directions. The speed, c , of these fronts is half the rate at which the pulse width is increasing, $c = \frac{1}{2} \frac{d\Phi}{dt} = \frac{1}{\alpha}(-\theta + G(\Phi))$. In the case of strictly excitatory coupling,

$$u_t = -u + \int_{-\infty}^{\infty} w_{ee}(x - x')H(u(x', t) - \theta)dx',$$

for which we have true traveling front solutions [4]; the threshold crossing point, a_f , and hence the front speed, c_f , can be tracked in a similar fashion:

$$c_f = \frac{da_f}{dt} = \frac{1}{\alpha} \left(-\theta + \int_0^\infty w(y)dy \right) = \frac{1}{\alpha}(-\theta + G(\infty)).$$

From this it is seen that the low-threshold destabilization of standing pulse solutions creates fronts with speeds asymptotically approaching those of true traveling fronts. This is a strictly formal argument, however, in that once stability is lost, $\alpha = \alpha(c)$ and can no longer be considered as constant.

4.2. Stability and the dynamics of inhibition.

4.2.1. Pulse width analysis. We now consider the system with more realistic inhibitory dynamics,

$$\begin{aligned} u_t &= -u + \int_{-\infty}^{\infty} w_{ee}(x - x')H(u(x', t) - \theta)dx' - \int_{-\infty}^{\infty} w_{ie}(x - x')v(x', t)dx', \\ (6) \quad \tau v_t &= -v + \int_{-\infty}^{\infty} w_{ei}(x - x')H(u(x', t) - \theta)dx', \end{aligned}$$

and derive an evolution equation describing the pulse width, providing a formal analysis of the dependence of stability on the speed of inhibition.

Starting from (6), we integrate the second equation to obtain

$$u_t(x, t) = -u(x, t) + w_{ee}(x) * H(u(x, t) - \theta) - L\{w_I * H(u(x, t) - \theta)\},$$

where $w_I(x) = w_{ie}(x) * w_{ei}(x)$ and L is the integral operator:

$$Lf(t) = \frac{1}{\tau} \int_{-\infty}^t e^{-(t-s)/\tau} f(s)ds.$$

Considering standing pulse solutions, we again define the points $a_j(t)$ ($j = 1, 2$) such that $u(a_j(t), t) = \theta$. Differentiating, we obtain

$$u_x(a_j, t) \frac{da_j}{dt} + u_t(a_j, t) = 0.$$

Approximating u_x by its steady state value and evaluating at $x = a_j$ leads to the evolution equations for $a_j(t)$,

$$\begin{aligned} \alpha \frac{da_1}{dt} &= \theta - W_E(a_2 - a_1) + L\{W_I(a_2 - a_1)\}, \\ \alpha \frac{da_2}{dt} &= -\theta + W_E(a_2 - a_1) - L\{W_I(a_2 - a_1)\}, \end{aligned}$$

where

$$\begin{aligned} W_E(x) &= \int_0^x w_{ee}(y) dy, \\ W_I(x) &= \int_0^x w_I(y) dy. \end{aligned}$$

As L is simply the convolution with a single exponential function, this is equivalent to a system of four differential equations:

$$\begin{aligned} \alpha \frac{da_1}{dt} &= \theta - W_E(a_2 - a_1) + z_1, \\ \tau \frac{dz_1}{dt} &= -z_1 + W_I(a_2 - a_1), \\ \alpha \frac{da_2}{dt} &= -\theta + W_E(a_2 - a_1) - z_2, \\ \tau \frac{dz_2}{dt} &= -z_2 + W_I(a_2 - a_1). \end{aligned}$$

Subtract the equations for a_j , define $\Phi \equiv a_2 - a_1$, and let $z = (z_1 + z_2)/2$ and $\zeta = (z_1 - z_2)/2$, to produce the third order system:

$$\begin{aligned} \alpha \frac{d\Phi}{dt} &= -\theta + W_E(\Phi) - z, \\ \tau \frac{dz}{dt} &= -z + W_I(\Phi), \\ \tau \frac{d\zeta}{dt} &= -\zeta. \end{aligned}$$

The last equation of the system is irrelevant, and the first two can be understood using phase-plane analysis. We comment in passing that this transformation has the effect of removing the translation invariance and corresponding zero eigenvalue as described in the next section.

The steady states of the planar system $\theta = W_E(\Phi) - W_I(\Phi)$ are the same as in section 3.1. The Jacobian evaluated at the fixed points is

$$J = \begin{pmatrix} W'_E(\Phi)/\alpha & -1/\alpha \\ W'_I(\Phi)/\tau & -1/\tau \end{pmatrix}.$$

The determinant is $\frac{1}{\tau\alpha}(W'_I(\Phi) - W'_E(\Phi))$ and the trace is $W'_E(\Phi)/\alpha - 1/\tau$. Thus the smaller root is a saddle point (since at this point $W'_I < W'_E$; see Figure 2a) while the

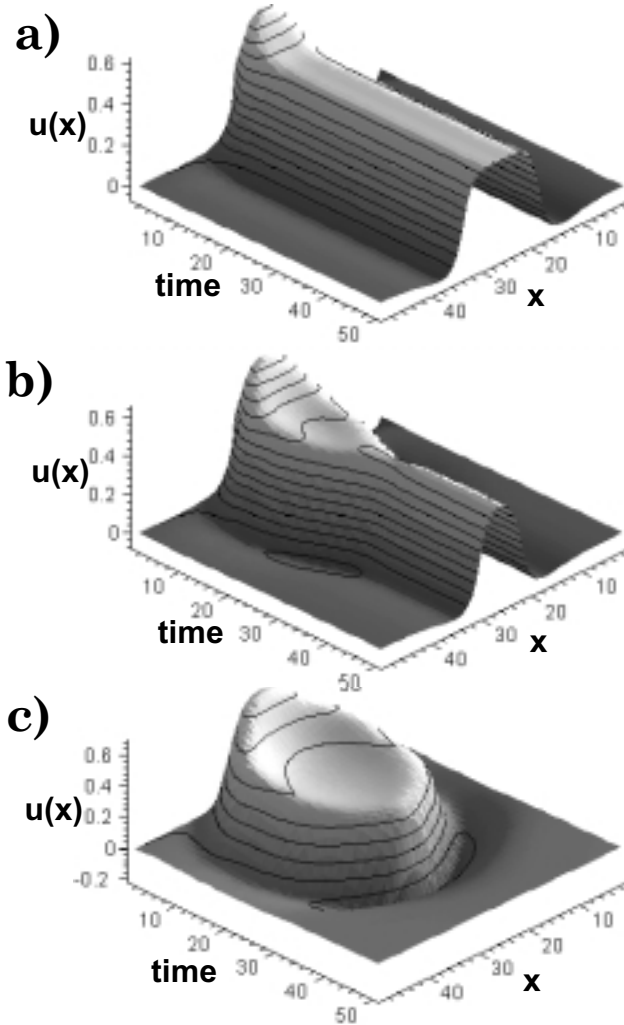


FIG. 4. *Dependence of pulse solutions on the speed of inhibition. Numerical solution of (2) with $w_{ee} = \frac{1}{2(.45)}e^{-\frac{|x|}{.45}}$, $w_{ei} = \frac{1}{2(.45)}e^{-\frac{|x|}{.45}}$, $w_{ie} = \frac{.7}{2(.62)}e^{-\frac{|x|}{.62}}$, and $P(U - \theta) = H(U - \theta)$ with $\theta = .2$. (a) $\tau = .4$, (b) $\tau = .55$, (c) $\tau = .7$. The initial condition is an instantaneous square pulse with an activity height of .3 (just above threshold) and a width of 10 spatial points. Note that stability of the pulse solution is lost as inhibition slows and that both the width and amplitude of the pulse show signs of oscillating near the bifurcation, indicative of an unstable periodic orbit.*

larger root is a node or vortex. The stability is determined by the trace. For large enough values of the time constant of inhibition, τ , the trace becomes positive so that the larger fixed point loses stability to a Hopf bifurcation, which will be discussed further in the following section.

We have used the software program AUTO [10] to compute the direction of bifurcation and, in all cases we have tried, the bifurcation is subcritical leading to unstable periodic fluctuations of the pulse. This differs from reaction-diffusion systems and may explain why we have not been able to obtain stable “breathing” pulse patterns in the full integral equations. Figure 4 presents a numerical example in which a stable

pulse loses stability as inhibition slows. Note the expanding and contracting pulse width near the bifurcation, indicating an unstable periodic orbit. We remark that these techniques can also be used to study the evolution of multiple pulses in the same domain.

4.3. Linear stability analysis. Let u_1 be a steady state pulse solution of (6) centered about the origin so that $a_2 = a$, $a_1 = -a$, and the pulse width $\phi = 2a$;

$$u_1 = (w_{ee} - w_{ie} * w_{ei}) * H(u_1 - \theta).$$

Linearizing (6) about u_1 leads to ($u \rightarrow z$, $v \rightarrow \psi$)

$$\begin{aligned} z_t &= -z + w_{ee} * (\delta(u_1 - \theta)z) - w_{ie} * \psi, \\ \tau\psi_t &= -\psi + w_{ei} * (\delta(u_1 - \theta)\psi), \end{aligned}$$

where δ is the Dirac delta function. We look for solutions of the form

$$\begin{aligned} z &= e^{\lambda t} z_1(x), \\ \psi &= e^{\lambda t} \psi_1(x), \end{aligned}$$

which thus satisfy

$$\begin{aligned} \lambda z_1(x) &= -z_1(x) + w_{ee} * (\delta(u_1 - \theta)z_1) - w_{ie} * \psi_1, \\ \lambda\tau\psi_1 &= -\psi_1(x) + w_{ei} * (\delta(u_1 - \theta)z_1). \end{aligned}$$

Solving for ψ_1 in the second equation, the first equation becomes

$$(7) \quad (1 + \lambda)z_1 = \left(w_{ee} - \frac{1}{1 + \lambda\tau} (w_{ie} * w_{ei}) \right) * (\delta(u_1 - \theta)z_1),$$

which, since $u_1(\pm a) = \theta$, becomes

$$(8) \quad \begin{aligned} (1 + \lambda)z_1 &= w_\tau * (\delta(u_1 - \theta)z_1) \\ &= \frac{1}{|u_1'(a)|} (w_\tau(x + a)z_1(-a) + w_\tau(x - a)z_1(a)), \end{aligned}$$

where, to simplify notation, we take

$$w_\tau \equiv w_{ee} - \frac{1}{1 + \lambda\tau} (w_{ie} * w_{ei})$$

and, for what follows,

$$w \equiv w_{ee} - (w_{ie} * w_{ei}).$$

Next we note that

$$\begin{aligned} u_1(x) &= w * H(u_1 - \theta) \\ &= \int_{-a}^a w(x - x') dx' = \int_{x-a}^{x+a} w(y) dy, \end{aligned}$$

so that

$$u_1'(x) = w(x + a) - w(x - a)$$

and (8) becomes

$$(9) \quad (1 + \lambda)z_1(x) = \frac{w_\tau(x+a)z_1(-a) + w_\tau(x-a)z_1(a)}{|w(2a) - w(0)|}.$$

Equality (9) implies

$$z_1(\pm a) = 0 \iff z_1(x) \equiv 0.$$

Hence we examine the matrix equation obtained from (9) at the points $x = \pm a$,

$$(1 + \lambda) \begin{pmatrix} z_1(a) \\ z_1(-a) \end{pmatrix} = \frac{1}{|w(0) - w(2a)|} \begin{pmatrix} w_\tau(0) & w_\tau(2a) \\ w_\tau(2a) & w_\tau(0) \end{pmatrix} \begin{pmatrix} z_1(a) \\ z_1(-a) \end{pmatrix},$$

whence it is seen that nontrivial solutions for $z_1(\pm a)$ (and hence $z_1(x)$) are possible only for those λ satisfying

$$1 + \lambda_\pm = \frac{w_\tau(0) \pm w_\tau(2a)}{|w(0) - w(2a)|}.$$

Expanding the eigenvalue equation,

$$\begin{aligned} (1 + \lambda_\pm\tau)(1 + \lambda_\pm) &= \frac{w_{ee}(0)(1 + \lambda_\pm\tau) - (w_{ie} * w_{ei})(0) \pm w_{ee}(2a)(1 + \lambda_\pm\tau) \mp (w_{ie} * w_{ei})(2a)}{|w(0) - w(2a)|} \\ &= \frac{\lambda_\pm\tau(w_{ee}(0) \pm w_{ee}(2a)) + w(0) \pm w(2a)}{|w(0) - w(2a)|}, \end{aligned}$$

we simplify to obtain

$$\lambda_\pm^2 + \left(1 + \frac{1}{\tau} - \frac{w_{ee}(0) \pm w_{ee}(2a)}{|w(0) - w(2a)|}\right) \lambda_\pm + \frac{1}{\tau} \left(1 - \frac{w(0) \pm w(2a)}{|w(0) - w(2a)|}\right) = 0.$$

We first consider the equation for λ_- . From the sketch of the LI kernel in Figure 1, note that $w(0) > w(2a)$, causing the last term to vanish. What remains,

$$\lambda_-^2 + \left(1 + \frac{1}{\tau} - \frac{w_{ee}(0) - w_{ee}(2a)}{|w(0) - w(2a)|}\right) \lambda_- = 0,$$

leads to the first two eigenvalues,

$$\begin{aligned} \lambda_- &= 0, \\ \lambda_- &= \frac{w_{ee}(0) - w_{ee}(2a)}{|w(0) - w(2a)|} - \left(1 + \frac{1}{\tau}\right). \end{aligned}$$

The first, $\lambda_- = 0$, is an expected result of the translation invariance of pulse solutions. The second provides the first condition for stability, namely,

$$(10) \quad \frac{w_{ee}(0) - w_{ee}(2a)}{|w(0) - w(2a)|} - \left(1 + \frac{1}{\tau}\right) < 0.$$

Similarly, we obtain an equation for λ_+ :

$$\lambda_+^2 + \left(1 + \frac{1}{\tau} - \frac{w_{ee}(0) + w_{ee}(2a)}{|w(0) - w(2a)|}\right) \lambda_+ + \frac{1}{\tau} \left(1 - \frac{w(0) + w(2a)}{|w(0) - w(2a)|}\right) = 0.$$

The eigenvalues λ_+ have negative real parts if and only if the coefficients of the quadratic are positive. If the constant coefficient is positive but the linear coefficient vanishes, then there are imaginary eigenvalues and we expect a Hopf bifurcation. The conditions for stability are thus

$$(11) \quad \frac{w(0) + w(2a)}{|w(0) - w(2a)|} < 1$$

and

$$(12) \quad \frac{w_{ee}(0) + w_{ee}(2a)}{|w(0) - w(2a)|} < \left(1 + \frac{1}{\tau}\right).$$

Note that, because $(w_{ee}(0) + w_{ee}(2a)) > (w_{ee}(0) - w_{ee}(2a))$, satisfying condition (12) is sufficient to satisfy condition (10).

What remains, then, are conditions (11) and (12). Condition (11) corresponds to Amari's original condition for the stability of the wide pulse. That is, $w(2a) < 0$; the value for the half-width a lies in the negative region of the lateral inhibition kernel. Condition (12) establishes the dependence of stability on τ , the time constant of inhibition.

Since, for the wide pulse, $w_{ee}(2a) - (w_{ie} * w_{ei})(2a) < 0$, we can establish the following inequalities:

$$w_{ee}(0) + w_{ee}(2a) > w_{ee}(0) - w_{ee}(2a) > (w_{ie} * w_{ei})(0) - (w_{ie} * w_{ei})(2a) > 0.$$

Expanding the denominator of (12),

$$\begin{aligned} & \frac{w_{ee}(0) + w_{ee}(2a)}{|(w_{ee}(0) - (w_{ie} * w_{ei})(0)) - (w_{ee}(2a) - (w_{ie} * w_{ei})(2a))|} \\ &= \frac{w_{ee}(0) + w_{ee}(2a)}{|(w_{ee}(0) - w_{ee}(2a)) - ((w_{ie} * w_{ei})(0) - (w_{ie} * w_{ei})(2a))|} \end{aligned}$$

reveals that the fraction is greater than one for the wide pulse. Thus, so long as τ is small (i.e., inhibition is fast), condition (12) holds. As inhibition slows, however, and τ increases, the condition is no longer satisfied and stability is lost. Since (12) implies that the linear term of the quadratic is positive, violation of this leads to loss of stability at a Hopf bifurcation. This suggests the possibility of a transition from a standing pulse to one with an oscillating width, i.e., a breathing pulse. In some reaction-diffusion systems, such solutions have in fact been found [28], [27]. As mentioned above, however, numerical analysis of the present system suggests the bifurcation is subcritical, leading to periodic solutions that are unstable.

5. Discussion. This study has examined the existence and stability of standing pulse solutions to an integro-differential equation system describing neuronal activity in a synaptically coupled network of excitatory and inhibitory neurons along a single spatial domain. Using the Heaviside function to describe firing rate, and assuming that inhibition acts instantaneously, Amari's formal analysis reveals the existence and stability of two standing pulse solutions, one wide and stable, the other narrow and unstable. However, the wide pulse becomes unstable through a Hopf bifurcation when more realistic inhibitory dynamics are incorporated. This is demonstrated using

both a formal argument that parallels Amari's approach and also through analysis of the linearized system. For more general firing rate functions, standing pulses are constructed using a singular perturbation argument. Interestingly, because both the inner and outer equations involve a spatial convolution, the matching criteria require consideration of global solutions from each layer. Other studies have also examined the existence and stability of standing pulses in similar systems using a fixed point theorem [20] and as a homoclinic solution to a similar set of convolution equations [5].

The present analysis does not support the hypothesis that sustained activity in prefrontal cortex is a result of the dynamics in an LI network [3], [2], [16]. However, no attempt was made to quantify the speed of inhibition necessary to maintain a stable pulse, and so the LI network mechanism cannot be ruled out completely. Anatomical studies have demonstrated the existence of direct long-distance inhibitory connections in prefrontal cortex [25], [23], and studies from other brain regions suggest that such connections can indeed play a functional role in organizing spatial activity [9]. However, in prefrontal cortex, fewer than 5% of long-distance connections synapse onto nonspiny neurons thought to be inhibitory in nature [25]. Those same neurons receive up to 25% of all synapses, both local and long-distance, suggesting that long-distance connections selectively target excitatory neurons [25]. On the other hand, inhibitory neurons in neocortex are strongly driven by excitatory input [35]. Thus, despite the paucity of direct connections, inhibition might still dominate over long distances via multi-synaptic pathways. While consistent with the underlying anatomy, this hypothesis introduces a delay to the onset of inhibition. Moreover, in contrast to the direct unit-to-unit connections in the Limulus retina, network inhibition in cortex is likely to require the integration of multiple inhibitory events, further accentuating the inhibitory delay [31], [19].

Alternative mechanisms that may explain sustained activity include the state-dependent bistability of individual neurons [22], [3]. Another possibility is that excitatory connections in prefrontal cortex are dominated by NMDA synapses, operating on a time scale much slower than GABA-mediated inhibition [32]. Finally, maintained activity might result from functional connections between the many brain regions exhibiting similar sustained activity patterns [6], [8], [26].

Acknowledgments. The authors wish to acknowledge Tasso Kaper and Eugene Wayne for their useful comments and criticisms.

REFERENCES

- [1] S. AMARI, *Dynamics of pattern formation in lateral-inhibition type neural fields*, Biol. Cybern., 27 (1977), pp. 77–87.
- [2] D. J. AMIT AND N. BRUNEL, *Model of global spontaneous activity and local structured activity during delay periods in the cerebral cortex*, Cereb. Cortex, 7 (1997), pp. 237–252.
- [3] M. CAMPERI AND X. J. WANG, *A model of visuospatial working memory in prefrontal cortex: Recurrent network and cellular bistability*, J. Comput. Neurosci., 5 (1998), pp. 383–405.
- [4] Z. CHEN, G. B. ERMENTROUT, AND B. MCLEOD, *Traveling fronts for a class of non-local convolution differential equations*, Appl. Anal., 64 (1997), pp. 235–253.
- [5] A. CHMAJ AND X. REN, *Homoclinic solutions of an integral equation: Existence and stability*, J. Differential Equations, 155 (1999), pp. 17–43.
- [6] J. D. COHEN, W. M. PERLSTEIN, T. S. BRAVER, L. E. NYSTROM, D. C. NOLL, J. JONIDES, AND E. E. SMITH, *Temporal dynamics of brain activation during a working memory task*, Nature, 386 (1997), pp. 604–608.

- [7] A. COMPTE, N. BRUNEL, P. S. GOLDMAN-RAKIC, AND X. J. WANG, *Synaptic mechanisms and network dynamics underlying spatial working memory in a cortical network model*, *Cereb. Cortex*, 10 (2000), pp. 910–923.
- [8] C. CONSTANTINIDIS AND M. A. STEINMETZ, *Neuronal activity in posterior parietal area 7a during the delay periods of a spatial memory task*, *J. Neurophys.*, 76 (1996), pp. 1352–1355.
- [9] J. M. CROOK, Z. F. KISVARDAY, AND U. T. EYSEL, *Evidence for a contribution of lateral inhibition to orientation tuning and direction selectivity in cat visual cortex: Reversible inactivation of functionally characterized sites combined with neuroanatomical tracing techniques*, *Eur. J. Neurosci.*, 10 (1998), pp. 2056–2075.
- [10] E. DOEDEL, (1999) *AUTO: Bifurcation and continuation numerical analysis software*. Available freely at <ftp://ftp.csconcordia.ca/pub/doedel/auto/>.
- [11] R. J. DOUGLAS, C. KOCH, M. MAHOWALD, K. A. C. MARTIN, AND H. H. SUAREZ, *The role of recurrent excitation in neocortical circuits*, *Science*, 269 (1995), pp. 981–985.
- [12] G. B. ERMENTROUT AND J. B. MCLEOD, *Existence and uniqueness of traveling waves for a neural network*, *Proc. Roy. Soc. Edinburgh. Sect. A*, 123 (1993), pp. 461–478.
- [13] G. B. ERMENTROUT, *Neural nets as spatio-temporal pattern forming systems*, *Rep. Progr. Phys.*, 61 (1998), pp. 353–430.
- [14] D. FERSTER AND K. D. MILLER, *Neuronal mechanisms of orientation selectivity in the visual cortex*, *Ann. Rev. Neurosci.*, 23 (2000), pp. 441–471.
- [15] C. D. GILBERT AND T. N. WIESEL, *Columnar specificity of intrinsic horizontal and corticocortical connections in cat visual cortex*, *J. Neurosci.*, 9 (1989), pp. 2432–2442.
- [16] P. S. GOLDMAN-RAKIC, *Cellular basis of working memory*, *Neuron*, 14 (1995), pp. 477–485.
- [17] B. S. GUTKIN, G. B. ERMENTROUT, AND O’SULLIVAN, *Layer 3 patchy recurrent excitatory connections may determine the spatial organization of sustained activity in the primate prefrontal cortex*, *Neurocomputing*, 32 (2000), pp. 391–400.
- [18] H. K. HARTLINE AND F. RATLIFF, *Inhibitory interaction in the retina of limulus*, in *Handbook of Sensory Physiology*, Vol. VII/2, Springer-Verlag, New York, 1972, pp. 381–447.
- [19] J. A. HIRSCH AND C. D. GILBERT, *Synaptic physiology of horizontal connections in the cat visual cortex*, *J. Neurosci.*, 11 (1991):1800–1809.
- [20] K. KISHIMOTO AND S. AMARI, *Existence and stability of local excitations in homogeneous neural fields*, *J. Math. Biol.*, 7 (1979), pp. 303–318.
- [21] Z. F. KISVARDAY, A. GULYAS, D. BEROUKAS, J. B. NORTH, I. W. CHUBB, AND P. SOMOGYI, *Synapses, axonal and dendritic patterns of GABA-immunoreactive neurons in human cerebral cortex*, *Brain*, 113 (1990), pp. 793–812.
- [22] J. E. LISMAN, J. M. FELLOUS, AND X. J. WANG, *A role for NMDA receptor channels in working memory*, *Nat. Neurosci.*, 1 (1998), pp. 273–275.
- [23] J. S. LUND AND D. A. LEWIS, *Local circuit neurons of developing and mature macaque prefrontal cortex: Golgi and immunocytochemical characteristics*, *J. Comp. Neurol.*, 328 (1993), pp. 282–312.
- [24] D. A. MCCORMICK, B. W. CONNORS, J. W. LIGHTHALL, AND D. A. PRINCE, *Comparative electrophysiology of pyramidal and sparsely spiny stellate neurons of the neocortex*, *J. Neurophysiol.*, 54 (1985), pp. 782–806.
- [25] D. S. MELCHITZKY, S. R. SESACK, M. L. PUCAK, AND D. A. LEWIS, *Synaptic targets of pyramidal neurons providing intrinsic horizontal connections in monkey prefrontal cortex*, *J. Comp. Neurol.*, 390 (1998), pp. 211–224.
- [26] E. K. MILLER, C. A. ERICKSON, AND R. DESIMONE, *Neural mechanisms of visual working memory in prefrontal cortex of the macaque*, *J. Neurosci.*, 16 (1996), pp. 5154–5167.
- [27] Y. NISHIURA AND M. MIMURA, *Layer oscillations in reaction-diffusion systems*, *SIAM J. Appl. Math.* 49 (1989), pp. 481–514.
- [28] J. E. RUBIN, *Stability, bifurcations and edge oscillations in standing pulse solutions to an inhomogeneous reaction-diffusion system*, *Proc. Roy. Soc. Edinburgh Sect. A*, 129 (1999), pp. 1033–1079.
- [29] D. C. SOMERS, S. B. NELSON, AND M. SUR, *An emergent model of orientation selectivity in cat visual cortical simple cells*, *J. Neurosci.*, 15 (1995), pp. 5448–5465.
- [30] J. S. TAUBE, R. U. MULLER, AND J. B. RANCK, JR., *Head-direction cells recorded from the postsubiculum in freely moving rats. I. Description and quantitative analysis*, *J. Neurosci.*, 10 (1990), pp. 436–447.
- [31] A. M. THOMSON AND J. DEUCHARS, *Temporal and spatial properties of local circuits in neocortex*, *Trends Neurosci.*, 17 (1994), pp. 119–126.
- [32] X. J. WANG, *Synaptic basis of cortical persistent activity: The importance of NMDA receptors to working memory*, *J. Neurosci.*, 19 (1999), pp. 9587–9603.

- [33] H. R. WILSON, B. KRUPA, AND F. WILKINSON, *Dynamics of perceptual oscillations in form vision*, *Nature*, 3 (2000), pp. 170–176.
- [34] H. R. WILSON AND J. D. COWAN, *A mathematical theory of the functional dynamics of cortical and thalamic nervous tissues*, *Kybernetik*, 13 (1973), pp. 55–80.
- [35] E. L. WHITE, *Cortical Circuits: Synaptic Organization of the Cerebral Cortex*, Birkhäuser, Boston, 1989.
- [36] J. XING AND G. L. GERSTEIN, *Networks with lateral connectivity. I. Dynamic properties mediated by the balance of intrinsic excitation and inhibition*, *J. Neurophysiol.*, 75 (1996), pp. 184–199.
- [37] K. ZHANG, *Representation of spatial orientation by the intrinsic dynamics of the head-direction cell ensemble: A theory*, *J. Neurosci.*, 16 (1996), pp. 2112–2126.